Silica Nanoparticles Dispersed in a Self-assembled Viscoelastic Matrix: Structure, Rheology, and Comparison to Reinforced Elastomers

Nicolas Puech, Serge Mora, Gregoire Porte, Isabelle Grillo, Ty Phou, Julian Oberdisse

Silica Nanoparticles Dispersed in a Self-assembled Viscoelastic Matrix: Structure, Rheology, and Comparison to Reinforced Elastomers

Nicolas Puech[1], Serge Mora[1], Grégoire Porte[1], Isabelle Grillo[2], Ty Phou[1], Julian Oberdisse[1,3 *]

[1] Laboratoire des Colloïdes, Verres, et Nanomatériaux (LCVN), Université Montpellier II, UMR CNRS 5587, 34095 Montpellier, France

[2] Institut Laue-Langevin (ILL), 6, rue Jules Horowitz, BP 156, 38042 Grenoble, France

[3] Laboratoire Léon Brillouin (LLB), CEA Saclay, UMR 12, 91191 Gif-sur-Yvette, France

Revised Manuscript

5th of September 2008

Abstract:

Model self-assembled networks of telechelic polymer C_{18}-PEO(35k)-C_{18} in water have been studied. The rheology of such transient networks has been investigated as a function of polymer concentration, and a typical percolation law has been observed. The network structure has been characterised by Small Angle Neutron Scattering in D_2O, where the interactions between micelles formed by the hydrophobic C_{18}-stickers of the polymer give rise to a peak in the scattered intensity. These model networks have then been used as a matrix for the incorporation of silica nanoparticles (R=10nm), and we have checked individual dispersion by scattering using contrast variation. The rheological response of the networks is considerably modified by the presence of the silica nanoparticles, and in particular an interesting dependence of the relaxation time on silica concentration has been found. The analogy in reinforcement behaviour of such a self-assembled, viscoelastic, and aqueous system with model experiments of elastomers filled with nanoparticles is discussed by comparison to a silica-latex system.

Figures: 9

(*) author for correspondence

I. Introduction

Reinforcement of elastomers with hard fillers is a common procedure for optimization of rheological or mechanical properties [1-6]. Many ways of incorporating the filler in the bulk polymer exist, the most popular being mechanical mixing. Other, usually more complex routes are in situ filler synthesis [5, 6], or polymerization around the filler particles[7-10]. It is commonly admitted that mechanical reinforcement depends on the state of dispersion of the filler particles, as well as on the interactions between the polymer matrix and the filler particles. The problem in many experimental systems resides in the fact that the dispersion of the nanoparticles is not a freely tuneable property, which impedes a detailed analysis of its contribution to reinforcement. Moreover, different filler surface treatments give not only different matrix-particle interactions, but also different particle dispersions.

As a first step of a systematic study of the reinforcement of elastic matrices, we have developed a silica-latex model system where the dispersion state of nanoparticles could be tuned with very little changes of the interfacial contribution [11-14]. This motivated research on different systems, where the interfacial contribution could be maintained at a constant level. Hydrogels may have this property, if the particles are hydrophilic and stable, which is why work on silica-filled oil-in-water microemulsion networks has been undertaken[15]. Such networks are made of microemulsion droplets stabilized by a surfactant and bridged by a triblock copolymer with hydrophobic end-groups called telechelic polymer, which sometimes micellizes also in absence of surfactant [16-29]. Very recently, networks of connected wormlike micelles have also attracted interest [29, 30]. In the case of the microemulsion networks, the interfacial contribution, however, was not found to be zero, due to weak attractive interactions between the surfactant molecules and the silanol groups on the silica surface [15, 31].

In this paper, a study of a pure (surfactant-free) triblock-copolymer system in water is presented, and its reinforcement properties by individually-dispersed silica nanoparticles are discussed in analogy with the silica-latex system. The experimental systems and methods are presented in section II, and we discuss experimental results concerning structure and rheology of filled telechelic hydrogels in section III, and compare them to model silica-latex elastomers, before concluding in section IV.

II. Model systems and experimental methods

II.1 Silica-latex nanocomposites: Here we describe the experimental setup already used in previous work [12]. An aqueous colloidal solution of a hydrophobic latex carrying a shell of ionisable groups of methacrylic acid for electrostatic stabilisation is mixed with a colloidal solution of silica particles. Due to the methacrylic acid, the latex particles carry a negative electric charge at high pH, as do the silica particles due to the silanol groups. The mixture is degassed and dried above the film formation temperature which is close to the glass transition temperature of the polymer. The polymer particles are then liquid drops which coalesce as the water is removed to form a continuous polymer film. Due to the presence of the ionisable groups, and to the silanol groups on the silica surface which have the same function of charge stabilisation, the structure of these solutions is pH- and electrolyte responsive. In practice, the silica nanoparticles (B30, R ≈ 10 nm) were incorporated in a latex matrix containing poly(methyl methacrylate) and poly(butyl acrylate) in such proportions that the glass transition temperature was set to 33°C. The initial radius of the latex particles was R = 14 nm.

II.2 Silica-telechelic hydrogels : Synthesis of the triblock copolymer CH_3-$(CH_2)_{17}$-NH-CO-O-$(CH_2$-CH_2-$O)_n$-CO-NH-$(CH_2)_{17}$-CH_3 has been described elsewhere [32, 33]. Here we study a 35k-poly(ethylene oxide) chain which has a hydrophobic C_{18}-sticker at each extremity, connected through a urethane group. The radius of gyration of the PEO-block is about 80 Å. Bindzil silica (B30/220, 30% wt) suspended in water was a gift from Akzo Nobel. The pH of the delivered stock solutions was set between 9 and 10 in order to ensure maximal colloidal stability to the silica by electrostatic repulsion. All silica-containing samples have thus been prepared at pH 10, all others at pH 7. The order of mixing of the components is of importance due to the high viscosity of the telechelic polymers networks. First we have prepared the sample containing silica nanoparticules and finally we add the telechelic copolymer. Two different batches have been used for the data shown in Figure 3 and all other plots.

II.3 Rheology: (a) Oscillatory shear experiments: Storage and loss moduli were determined as a function of ω in the linear regime (low amplitudes, γ = 10%), and we have checked linearity up to 20%. As with the data presented in the literature, G' and G'' of telechelic polymer networks show essentially Maxwellian behaviour, i.e. they can be characterized by a modulus G and a single relaxation time. Minor deviations from Maxwellian behavior are discussed later in the article. (b) Stretching: The mechanical properties of silica-latex

nanocomposites have been tested by uniaxial stress-strain isotherms. The reference case for the mechanical tests was given by the stress-strain isotherms of the pure latex films. These were found to depend strongly on pH, which is why the reinforcement factor presentation was chosen to highlight the filler contribution to the stress. This presentation consists in normalising at each deformation the nanocomposite stress by the stress of the pure latex sample at the same pH, $\sigma(\lambda)/\sigma_{latex}(\lambda)$. It thus answers the question, how much stronger the composite with respect to its own matrix is.

II.4 Small Angle Neutron Scattering (SANS): Scattering experiments have been performed on beamline PACE at LLB (Saclay) and on the beamline D11 at ILL (Grenoble). The configurations were (1m and 4.68 m at 6Å; 4.68 m at 13Å) at LLB and (1.2m, 5m, 20m at 6Å; 34m at 10 Å) at ILL. Samples have been prepared in D_2O, small quantities of H_2O from the silica stock solution have been accounted for in the calculation of the solvent scattering length densities. Empty cell scattering has been subtracted, and detector efficiency has been corrected as usual with light water. Data were normalized either by an empty beam measurement (LLB), or by using beamline constants determined from standards (ILL). The incoherent background substraction was performed by comparing to Porod scattering expected for smooth interfaces.

III. Results

III.1 Silica-latex nanocomposites

Several papers have been published on the silica-latex model system, and in particular on the structure of the silica in this particular polymer matrix [34, 35] . For the sake of comparison with the hydrogel system, important results are recalled and put into perspective.

The structure of the silica nanoparticles in the matrix results from the colloidal interactions, mainly electrostatics and Van der Waals, in solution before film formation. Experimentally, the structure is accessible by Small Angle Scattering, e.g. of neutrons, which essentially see a binary contrast between particles and matrix. The scattering signal can then be decomposed in a form and structure factor contribution, where the form factor can be measured independently using highly dilute silica stock solutions. The scattering experiment allows thus to access directly the structure factor, which is nothing but the Fourier transform of the pair

correlation functions of the silica particles. Detailed analysis of the scattering data has been performed in the past [35], and the following, simplified picture was found to be compatible with the scattering experiment: Silica particles, which interact mainly through electrostatic repulsion, carry more electrostatic charges at higher pH in solution. This mechanism leads to a better dispersion of the nanoparticles in the polymer matrix, i.e. less aggregation, at high pH of the precursor solution. At lower pH (down to 4), the particles tend to aggregate in clusters of several thousands, which leads to very strong forward scattering. At intermediate solution pH, around 7, particles aggregate in clusters of approximately one hundred, but the remaining repulsion between particles induces a strong liquid-like ordering of the clusters within the matrix. This leads to a characteristic peak in q-space, the position of which can be used to estimate the average aggregation number with good precision; in any event, such a structure is compatible with the scattering data, as shown by Reverse Monte Carlo simulations [35].

In Figure 1, the mechanical response of the silica-latex nanocomposites is plotted as a function of elongation $\lambda = L/L_o$, where L and L_o are sample length and initial length, respectively. This data has been already reported in ref. [11]. The mechanical response is expressed in terms of the reinforcement factor, obtained by dividing the stress of the nanocomposite by the stress of the pure matrix made at identical pH, σ/σ_{latex}. The samples chosen contain all 5%v of silica nanoparticles, but the preparation pH has been varied (about 4, 7, 9, called 'acid', 'neutral', and 'basic'). The aggregation numbers indicated in the plot have been determined from the peak positions of the scattered intensities. It is clear from Figure 1, that the reinforcement factor, which tells us how much stronger the nanocomposite is with respect to the pure matrix, depends strongly on the state of dispersion of the nanoparticles. In particular, higher aggregation leads to considerably stronger reinforcement, especially at low λ where Young's modulus is probed. At higher deformations, the reinforcement factor decreases in all cases, but stays still superior in the case of the low-pH samples. A simple interpretation of this λ-dependence is that big aggregates contribute strongly to reinforcement, and that they break up under deformation, thereby reducing the reinforcement factor of the composites [36]. At large deformation, finally, only small aggregates and potentially slightly different interfacial interactions contribute to the reinforcement.

This analysis of the reinforcement factor emphasises the fact that in silica-latex nanocomposites the contribution of the interface is if not constant, at least negligible with respect to the contribution of the structure or nanoparticle dispersion. On the other hand, the dominant influence of the structure is clearly visible, as smaller aggregates contribute less to the reinforcement. Such considerations have motivated the study of a completely different system, based on water-soluble polymer network structures, where it was thought that the nanoparticles can be individually dispersed in the solvent, with little or no interaction with the polymer. As indicated in the introduction, a first system, based on a microemulsion connected with telechelic polymer, has proven to interact with the silica due to formation of surfactant micelles on the silica surface [15]. In this paper, we present new experimental evidence for a surfactant-free transient network system. It displays interesting rheological properties, which are further enhanced by addition of silica nanoparticles.

III.2 Silica-telechelic hydrogels

The phase behaviour of telechelic copolymer C_{18}-PEO(35k)-C_{18} in water has been studied at 22°C. In Figure 2, the system is seen to phase separate at low volume fractions, and to present a homogeneous phase above Φ_p = 2.5%. This homogeneous phase is transparent and colourless, and upon simple visual inspection viscoelastic properties are found. Note that in microemulsion systems, a fluid monophasic domain made of 'flowers' (unconnected copolymer micelles) is usually found at very low volume fractions [37], but this was not the scope of the present study. If we add silica nanoparticles in aqueous solution, at a fixed polymer volume fraction of Φ_p = 3% and at a pH of the mixture of 10 to ensure nanoparticle dispersion, the system stays monophasic up to silica volume fractions of Φ_{si} = 8%, and flocculates above. We have determined typical sizes and distances by Small Angle Neutron Scattering, cf. below, and in Figure 2 the result of this analysis is sketched on the right-hand side. The dense transient network of the copolymer is made of rather small hydrophobic domains (the nodes), connected by the PEO-chains. The silica particles, although of nanometric size (R = 100 Å), are embedded in this network, and positioned at typical distances of 400 Å.

The rheological properties of the pure copolymer network in water have been studied as a function of polymer volume fraction Φ_p in the monophasic region (cf. Fig. 2) by small

amplitude oscillatory shear experiments and flow curves $\sigma(\dot{\gamma})$. The oscillatory shear experiments, performed in the linear domain (ω = 1 - 300 rad s^{-1}, γ = 10%), give access to G' and G'', whereas the flow curves yield the viscosity η. A Maxwell model was fitted to G' and G''(ω), giving the plateau modulus G and the relaxation time τ, cf. ref. [15] for details. The main results are summarized in a single plot as a function of polymer volume fraction Φ_p in Figure 3. The outcome of the two experiments, oscillatory shear and flow, is coherent within errorbars, as the viscosity of a Maxwell fluid is also given by $\eta = G\,\tau$. Unlike the treatment in terms of a percolation model suitable for the connected microemulsion model, the existence of a phase separation does not allow us to use such a model over the complete concentration range. We have nonetheless tempted a percolation fit on the modulus, the relaxation time, and the viscosity, and obtain the following equations:

$$\begin{aligned} G &= 2200\ \text{Pa}\ \ [(\Phi_p - 0.02)/0.02]^{0.8} \\ \tau &= 0.022\ \text{s}\ [(\Phi_p - 0.02)/0.02]^{0.55} \\ \eta &= 60\ \text{Pa s}\ [(\Phi_p - 0.02)/0.02]^{1.35} \end{aligned} \qquad (1)$$

The critical value characterizing the onset of percolation in polymer volume fraction, 0.02, is found to be identical for all three quantities. It is located within the two-phase region, which is expected given that the monophasic region has gel properties up to the phase boundary. The prefactors and the exponent satisfy the relationship for Maxwell fluids quite well, as the product of the prefactors of modulus and relaxation time is comparable to the one of the viscosity, and the exponents add up. For further comparison, keep in mind that the data in Fig. 3 have been obtained with a different polymer batch, but all observed tendencies are robust.

The changes in the rheological properties of the copolymer network at Φ_p = 3% upon addition of silica nanoparticles have been measured following the same experimental protocol. As it will be shown below, the network still shows a dominant single relaxation time, with a minor second contribution in presence of silica. We have thus fitted G' and G''(ω) as before, and in Figure 4 the resulting modulus G is plotted as a function of silica volume fraction. The modulus is found to increase by about 30% in the observed range, and a linear fit gives G = 2300 Pa (1 + 5.2 Φ_{si}).

In Figure 5, the relaxation time τ determined through the Maxwell fit is represented as a function of silica content. This quantity is found to increase considerably, by more than 50% in the observed range, and a linear fit gives $\tau = 0.02$ s $(1 + \Phi_{si})$. Such a behaviour is striking. In particular, we have previously observed in filled microemulsion networks that the relaxation time decreases with silica volume fraction, proportional to $(1\text{-}2\Phi_{si})$. The interpretation of this peculiar behaviour is unclear at the moment, and probably related to differences in the microstructure. The PEO chains may interact through hydrogen bonding with the negatively charged silica surface (high pH). The energetic barrier, however, would be of the order of kT for one such bond, thus very small with respect to the energy necessary to pull out a C_{18}-sticker out of a hydrophobic domain. An alternative explanation might be that the silica particles sterically hinder reorganisation of the polymer molecules, and thus relaxation. In other words, a sticker leaving a micelle might not be able to reach another micelle, and might return to its original state of stress. To solve this issue, experiments as a function of temperature might give further hints on the physical origin of the slow down of this relaxation mode.

Due to the growth in both G and τ, the viscosity increases even more with silica volume fraction. This is shown in Figure 6, where the experimental viscosity is plotted in reduced units ("reinforcement factor") as a function of Φ_{si}. This representation allows a direct comparison to the Einstein prediction $(1+ 2.5\ \Phi_{si})$ [38]. The experimental data indicates a much stronger Φ_{si}-dependence, clearly incompatible with the purely hydrodynamic Einsteinian reinforcement. On may wonder if this is due to the electrostatic interactions between silica particles in solution. In a control experiment, we have measured the viscosity of pure silica solutions at the same pH (10), and the fit to this data is shown in Figure 6 (dotted line) for comparison. Given the much stronger rheological response of the filled copolymer network, with a viscosity reinforcement of more than a factor of two, one can again only speculate on the physical origin of this effect.

We now come back to the existence of a second relaxation time in the silica-filled copolymer network. Experimental evidence is plotted in Figure 7, where G' and G''(ω) with and without silica filler are compared. In the pure copolymer network, the Maxwellian fit is satisfactory, whereas a mismatch at low frequencies was observed in the silica-filled system. For the sake

of clarity, only the calculation for G'(Φ_{si}=0.0654, single mode) is shown in Figure 7 as illustration of the mismatch (solid line). G' and G'' for both systems have been fitted with a model expression with two relaxation times (dotted lines), and thus four parameters in total, all given in the figure caption. The corresponding fit is seen to be much better at low frequencies, for all data, although essentially the same relaxation times were used for the fits (0.2 s and 0.032 s). Note that due to the weakness of the effect, the choice of the parameters of the slower mode is not unambiguous, and several couples (G_2, τ_2) may be found. They all have in common, however, that G_2 is much smaller than G_1, and τ_2 much larger than τ_1. It is also clear from these parameters (low G_2) that the silica-free network does not need a second mode for a proper description.

As indicated in Figure 2, we have quantitative information on the structure of the telechelic gel filled with silica nanoparticles. We start with the structure of the pure hydrogel at a copolymer volume fraction of Φ_p = 2% in D_2O. The change in solvent is necessary to highlight the polymer in Small Angle Neutron Scattering. As usual, it slightly shifts the phase boundaries, and the 2% sample in D_2O was monophasic and in a gel state. In Figure 8, the scattering cross section I(q) is plotted as a function of wavevector q. Three different scattering regimes are found. At low q, the intensity decreases roughly proportional to $1/q^2$. This low-q behaviour is related to the concentration fluctuations of the copolymer, whose hydrophobic blocks constantly form and break-up small micellar regions. Around $q_o \approx 0.02$ Å^{-1}, a prominent correlation peak can be seen, which we interpret as the signature of the positional correlations between the small micellar regions. From the properties of the Fourier transformation, a typical average distance of $2\pi/q_o \approx 320$ Å between centers of micelles can be deduced. The number of micelles per unit volume is thus 3.10^{16} cm^{-3}, whereas the number of polymer molecules at 2%v is $3.4\ 10^{17}$ cm^{-3}. Eleven molecules or 22 stickers thus participate in the formation of an average micelle. Using the typical size of a hydrophobic C_{18}-sticker, we can estimate the volume of a hydrophobic domain to V ≈ 10000 Å^3, which corresponds to a radius of 13 Å. The form factor scattering of these hydrophobic regions would start at approximately $I_o = \Phi_h\ \Delta\rho^2\ V$, which is very low (0.1 cm^{-1}, with the volume fraction of the hydrophobic region $3\ 10^{-4}$, and the contrast estimated to $5\ 10^{10}$ cm^{-2}) compared to the observed signal. The entire chain thus contributes to the scattering, and an analogous calculation for the form factor scattering of a single chain gives 3 cm^{-1}. At high q, finally, a scattering law typical for chains in good solvent is found ($I \alpha q^{-1.7}$). It must be emphasized that the typical sizes clearly visible in

neutron scattering and the equally well-known chain characteristics appear to be in contradiction, as the radius of gyration is considerably smaller than the average distance between objects. Chains do not appear to be stretched on average, if one trusts the high-q behaviour. A consistent picture would be that only a fraction of chains is stretched to connect the hydrophobic domains, whereas the others are present as loops or dangling ends. Concerning this latter hypothesis, it may be noted that the hydrophobic domains, which are rather small, fluctuate constantly, possibly up to complete disintegration, and that single stickers may be found in solution (dangling ends).

The second scattering curve plotted in Figure 8 represents the structure of the copolymer network containing index-matched (and thus invisible) silica particles. The intensity has been rescaled to compensate the difference in scattering length density of the solvent, and the good superposition at large-q shows that the chains obey the same chain statistics (good solvent). The difference in the low-q scattering (an apparent $q^{-1.1}$ power-law) and the slight shift in the peak position indicate that the positional correlations between the hydrophobic domains have been perturbed by the presence of the silica particles. This is to be expected, given the crowded environment created by the silica particles, as we have sketched it in Figure 2. Note that there is no straightforward interpretation for the low-q scattering laws in absence or presence of silica. The only sure fact is the absence of a low-q scattering plateau, which indicates that there are concentration fluctuations involving many molecules.

As a last point, we now discuss the dispersion of the silica in the copolymer network. Unfortunately, we do not have a complete data set on the same system. In Figure 9, scattered intensities collected on a very similar system, made of small micelles connected by the same 35k-copolymer are shown. In this case, the small micelles have been indexed-matched, and only the silica contributes to the scattering. In a second experiment, the pure silica was measured in solution independently, and the two data sets have been rescaled to identical contrast conditions. As can be seen from the very good superposition of the intensities, the silica in the copolymer network is dispersed just as well as it is dispersed in pure solvent. The same result was found for the 35k-silica system, where the scattering was measured only at intermediate angles, and good superposition obtained. In conclusion, this proves that the silica particles are individually dispersed at these high pH values.

If we collect all the information obtained by rheology and scattering, it appears that there is a specific effect of the silica nanoparticles on the flow properties of the copolymer network. Due to their electrostatic charge, the nanoparticles are suspended individually in the network in exactly the same way they are suspended in pure water. On the other hand, the configurations of the copolymer molecules are clearly seen to be affected by the addition of the particles. It is unclear at the moment, if this effect is due to interactions between the polymer and the silica, or if the simple presence of the silica forces the polymer to reorganize spatially. In any event, important rheological changes are observed, and must be related to the modified polymer microstructure, as evidenced by SANS.

IV. Conclusions and outlook

We have investigated and compared two very different nanocomposites. One is typical for elastomer reinforcement, where hard silica particles are dispersed in a latex polymer matrix. The other is a hydrogel, thus containing solvent, and silica particles suspended in the solvent. In the silica-latex system, mechanical reinforcement has been measured for different states of aggregation, for more or less identical polymer-silica interactions. This allows us to identify the contribution of the filler structure to the reinforcement effect. The second system was designed to investigate the influence of structure in a similar way, and in this article a first series of results on a pure (surfactant-free) copolymer network with individually dispersed silica particles is presented. When comparing the reinforcement effect for similar silica volume fractions (5%-7%) in the two systems, it appears that it is of the same order of magnitude for low aggregation numbers. In both cases, the contribution is stronger than the Einstein prediction, and also stronger than the viscosity increase of a pure silica solution. In the case of the silica-latex nanocomposites, the origin of the effect is thought to be due to interfacial interactions, whereas in the hydrogels the situation is more complicated. In particular, it is not clear if the adsorption of copolymer onto the silica shall be viewed as an interfacial modification or a change in network connectivity. In future work, it will be interesting to create hydrogels filled with aggregated silica particles to allow for a full comparison.

It is interesting to put the observed reinforcement in the context of the most fundamental reinforcement laws. Einstein's prediction $\eta = \eta_o (1+2.5\ \Phi)$ holds for a purely viscous flow around an isolated spherical particle [38]. In the other extreme, Smallwood has shown that

Einstein's prediction applies also to the reinforcement of the modulus of a purely elastic solid [39]. In our case, we have measured both the modulus (Fig; 4) and the viscosity (Fig. 6) of a viscoelastic reinforced system. Note that the modulus corresponds to what would have been measured in a step-strain experiment, i.e. it is measured in absence of relaxation of the samples. As a result, it seems that we can both apply Smallwood's equation to the modulus, and Einstein's equation to the viscosity. However, as the viscosity is given by the product of the modulus and the relaxation time, this can only work if the relaxation time is constant. In this article, we have provided evidence that this is not always the case, and that specific interactions can slow down (or speed up[15]) the relaxation time. This introduces an additional dependence on particle volume fraction, not taken into account in the original theories.

A possible extension of this system is to vary the structure of the silica particles, by decreasing the pH and thus the electrostatic interactions between nanoparticles. This can be done in close analogy with the study of the silica-latex nanocomposites, where the aggregation numbers could be varied from a few to several thousands. It is unclear if a good control of monodispersity can be obtained using a similar protocol (pH changes); nonetheless, it would allow to conclude independently on the contributions of filler structure, and specific filler-matrix interactions, some evidence of which has been reported on in this paper.

Acknowledgements: Work conducted within the scientific program of the European Network of Excellence *Softcomp*: 'Soft Matter Composites: an approach to nanoscale functional materials', supported by the European Commission. Silica stock solutions were a gift from Akzo Nobel.

References:

1 J. E. Mark, B. Erman and F. R. Eirich, *Science and Technology of Rubber*, Academic Press, San Diego, 1994.

2 D. C. Edwards, *J Mat Sci*, 1990, **25**, 4175.

3 A. I. Medalia, *Journal of Colloid and Interface Science*, 1970, **32**, 115-131.

4 A. Voet, *Macromolecular Reviews Part D-Journal of Polymer Science*, 1980, **15**, 327-373.

5 D. W. McCarthy, J. E. Mark, S. J. Clarson and D. W. Schaefer, *Journal of Polymer Science Part B-Polymer Physics*, 1998, **36**, 1191-1200.

6 D. W. McCarthy, J. E. Mark and D. W. Schaefer, *Journal of Polymer Science Part B-Polymer Physics*, 1998, **36**, 1167-1189.

7 Z. C. Pu, J. E. Mark, J. M. Jethmalani and W. T. Ford, *Chemistry of Materials*, 1997, **9**, 2442-2447.

8 J. Berriot, F. Lequeux, H. Montes and H. Pernot, *Polymer*, 2002, **43**, 6131-6138.

9 J. Berriot, F. Martin, H. Montes, L. Monnerie and P. Sotta, *Polymer*, 2003, **44**, 1437-1447.

10 J. Berriot, H. Montes, F. Martin, M. Mauger, W. Pyckhout-Hintzen, G. Meier and H. Frielinghaus, *Polymer*, 2003, **44**, 4909-4919.

11 J. Oberdisse, *Macromolecules*, 2002, **35**, 9441-9450.

12 J. Oberdisse and B. Deme, *Macromolecules*, 2002, **35**, 4397-4405.

13 J. Oberdisse, A. El Harrak, G. Carrot, J. Jestin and F. Boue, *Polymer*, 2005, **46**, 6695-6705.

14 J. Oberdisse, *Soft Matter*, 2006, **2**, 29-36.

15 N. Puech, S. Mora, V. Testard, G. Porte, C. Ligoure, I. Grillo, T. Phou and J. Oberdisse, *EPJE*, 2008, **DOI: 10.1140/epje/i2007-10275-3**.

16 T. Annable, R. Buscall, R. Ettelaie and D. Whittlestone, *Journal Of Rheology*, 1993, **37**, 695-726.

17 G. Fleischer, F. Stieber, U. Hofmeier and H. F. Eicke, *Langmuir*, 1994, **10**, 1780-1785.

18 D. Vollmer, J. Vollmer, B. Stühn, E. Wehrli and H. F. Eicke, *Physical Review E*, 1995, **52**, 5146.

19 M. Odenwald, H. F. Eicke and W. Meier, *Macromolecules*, 1995, **28**, 5069-5074.

20 M. Filali, R. Aznar, M. Svenson, G. Porte and J. Appell, *Journal of Physical Chemistry B*, 1999, **103**, 7293-7301.

21 B. Xu, L. Li, A. Yekta, Z. Masoumi, S. Kanagalingam, M. A. Winnik, K. W. Zhang and P. M. Macdonald, *Langmuir*, 1997, **13**, 2447-2456.

22 H. BaggerJorgensen, L. Coppola, K. Thuresson, U. Olsson and K. Mortensen, *Langmuir*, 1997, **13**, 4204-4218.

23 E. Michel, M. Filali, R. Aznar, G. Porte and J. Appell, *Langmuir*, 2000, **16**, 8702-8711.

24 F. Molino, J. Appell, M. Filali, E. Michel, G. Porte, S. Mora and E. Sunyer, *Journal of Physics-Condensed Matter*, 2000, **12**, A491-A498.

25 F. E. Antunes, K. Thuresson, B. Lindman and M. G. Miguel, *Colloids and Surfaces a-Physicochemical and Engineering Aspects*, 2003, **215**, 87-100.

26 P. Kujawa, H. Watanabe, F. Tanaka and F. M. Winnik, *European Physical Journal E*, 2005, **17**, 129-137.

27 G. Porte, C. Ligoure, J. Appell and R. Aznar, *Journal of Statistical Mechanics-Theory and Experiment*, 2006.
28 Y. Serero, V. Jacobsen, J. F. Berret and R. May, *Macromolecules*, 2000, **33**, 1841-1847.
29 T. P. Lodge, R. Taribagil, T. Yoshida and M. A. Hillmyer, *Macromolecules*, 2007, **40**, 4728-4731.
30 L. Ramos and C. Ligoure, *Macromolecules*, 2007, **40**, 1248-1251.
31 G. Despert and J. Oberdisse, *Langmuir*, 2003, **19**, 7604-7610.
32 D. Calvet, A. Collet, M. Viguier, J. F. Berret and Y. Serero, *Macromolecules*, 2003, **36**, 449-457.
33 J. P. Kaczmarski and J. E. Glass, *Macromolecules*, 1993, **26**, 5149-5156.
34 J. Oberdisse, Y. Rharbi and F. Boue, *Computational and Theoretical Polymer Science*, 2000, **10**, 207-217.
35 J. Oberdisse, P. Hine and W. Pyckhout-Hintzen, *Soft Matter*, 2007, **2**, 476-485.
36 H. Luo, M. Kluppel and H. Schneider, *Macromolecules*, 2004, **37**, 8000-8009.
37 M. Filali, M. J. Ouazzani, E. Michel, R. Aznar, G. Porte and J. Appell, *Journal of Physical Chemistry B*, 2001, **105**, 10528-10535.
38 A. Einstein, *Ann. Phys.*, 1906, **19**, 289.
39 H. M. Smallwood, *J Appl Phys*, 1944, **15**, 758-766.

Figure Captions:

Figure 1: Reinforcement factor of silica-latex nanocomposites (Φ_{si} = 5%, three samples at pH ca. 4, 7 and 9), as a function of relative elongation $\lambda = L/L_o$. The average aggregation numbers have been measured by Small Angle Neutron Scattering, see text for details.

Figure 2: (a) Phase diagram of 35k copolymer in water for increasing polymer volume fraction Φ_P at pH 10. (b) Phase diagram of 35k copolymer in water at Φ_P =3% for increasing silica volume fraction at pH 10. (c) Schematic view of transient copolymer network.

Figure 3: Modulus G in Pa, τ in s and η in Pa.s of 35k copolymer network as a function of polymer volume fraction Φ_P.

Figure 4: Modulus G in Pa of filled 35k copolymer network (Φ_P =3%) for increasing silica volume fraction Φ_{Si}. All samples are at pH 10.

Figure 5: Relaxation time in s of filled 35k copolymer network (Φ_P =3%) for increasing silica volume fraction Φ_{Si}. All samples are at pH 10.

Figure 6: Viscosity in Pa.s of filled 35k copolymer network (Φ_P =3%) for increasing silica volume fraction Φ_{Si}. Data is compared to the viscosity of a pure silica solution (solid line) and to the Einstein prediction (dotted line). All samples are at pH 10.

Figure 7: Storage G'(Pa) (●) and loss G''(Pa) (■) modulus as a function of ω of (a) a filled 35k copolymer network (Φ_P = 3%, Φ_{si} = 6.54%) compared with a copolymer network without silica G'(Pa) (○) and loss G''(Pa) (□) (Φ_P = 3%, Φ_{si} = 0%). With silica, departures from Maxwellian behaviour are emphasized in G" at high ω, and in G' at low ω, which is illustrated by the solid line

calculated for G' with silica, using a single relaxation time (G_1 = 3200 Pa; τ_1 = 0.032 s). The dottted lines are fits with a double Maxwell model G_1 = 3200 Pa; G_2 = 140 Pa τ_1 = 0.032 s; τ_2 = 0.2 s for the filled network and G_1 = 2400 Pa; G_2 = 15 Pa; τ_1 = 0.024 s; τ_2 =0.2 s for the pure network.

Figure 8: Scattered intensity I in cm^{-1} as a function of wave vector q in $Å^{-1}$ in pure D_2O of 35k copolymer network with a volume fraction Φ_P = 2% (●). The data is compared to the intensity of the same network containing 6.54%v of index matched silica particles (□, $\rho_{solv} = \rho_{Si} = 3.5.10^{10}$ cm^{-2}). The latter intensity has been rescaled to the one of the pure copolymer in order to compensate the differences in contrast.

Figure 9: Scattered intensity I in cm^{-1} as a function of wave vector q in $Å^{-1}$ of filled 35k networks containing contrast-matched microemulsion (○, Φ_{si} = 6%, R = 30 Å, 4%, $\rho_{solv} = \rho_m = 0.3.10^{10}$ cm^{-2}). This is compared to the intensity of pure silica (●) at the same volume fraction, rescaled to identical contrast conditions.

Figures

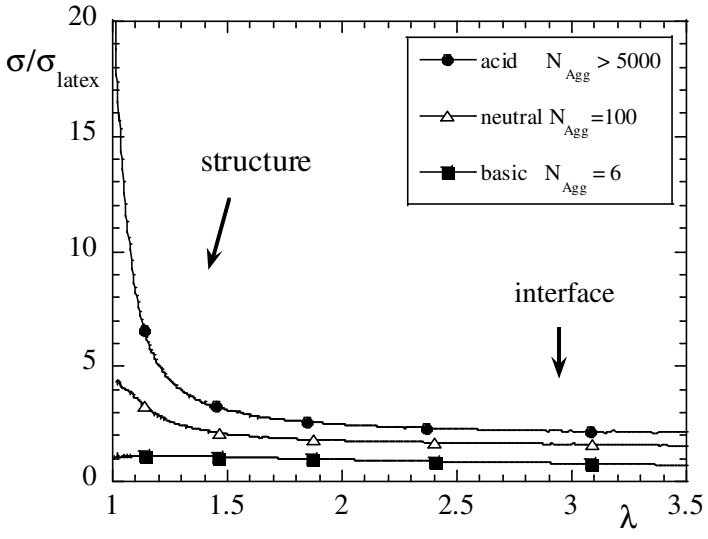

Figure 1 (Puech et al)

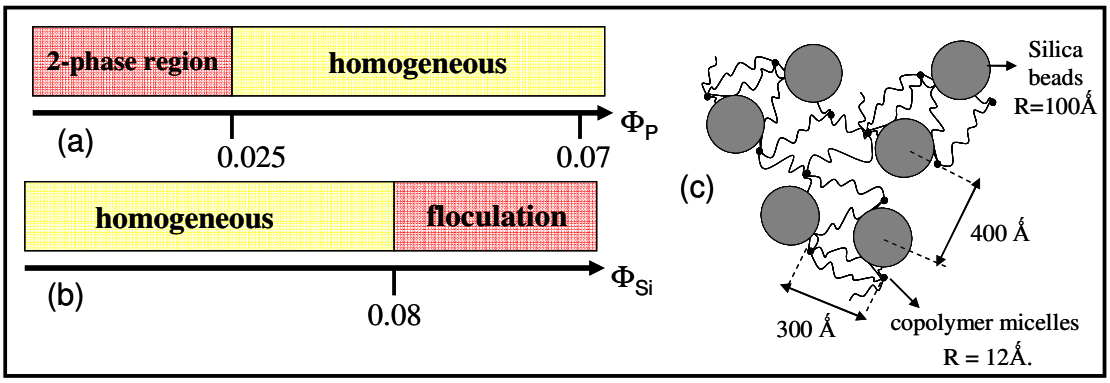

Figure 2 (Puech et al)

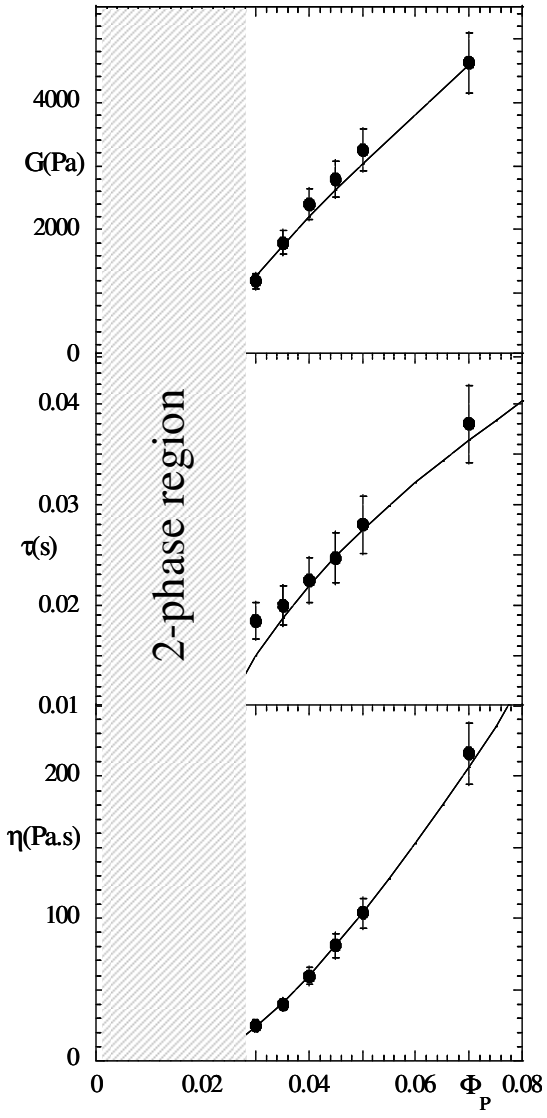

Figure 3 (Puech et al)

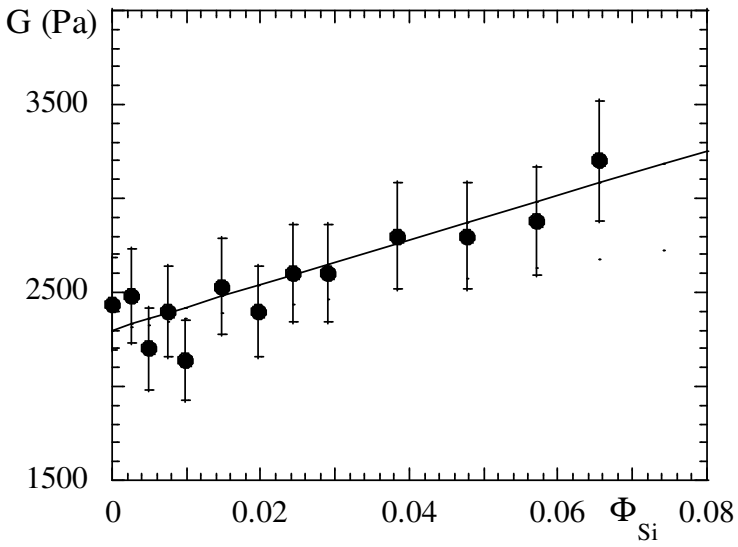

Figure 4 (Puech et al)

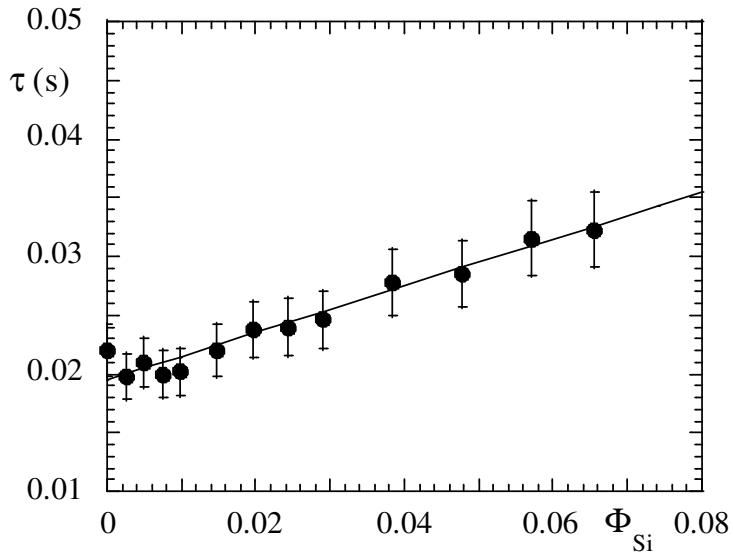

Figure 5 (Puech et al)

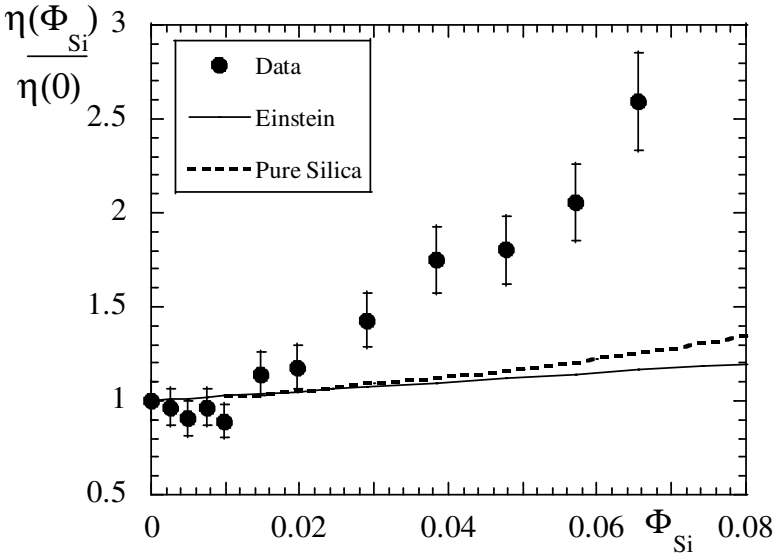

Figure 6 (Puech et al)

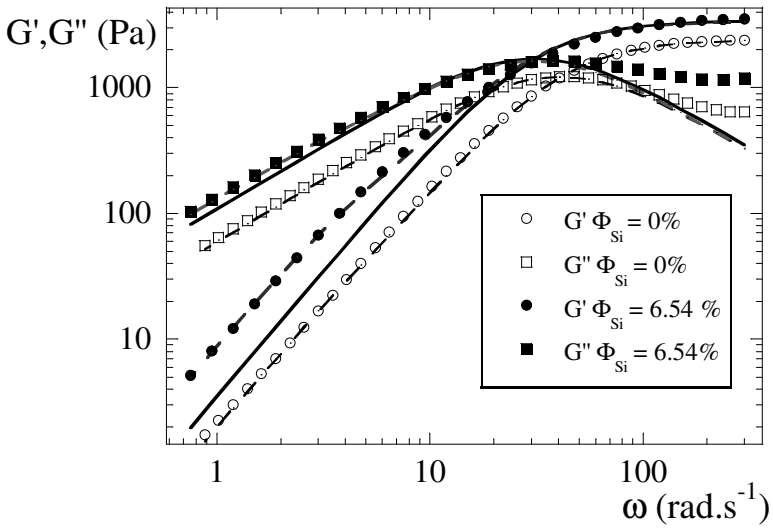

Figure 7 (Puech et al)

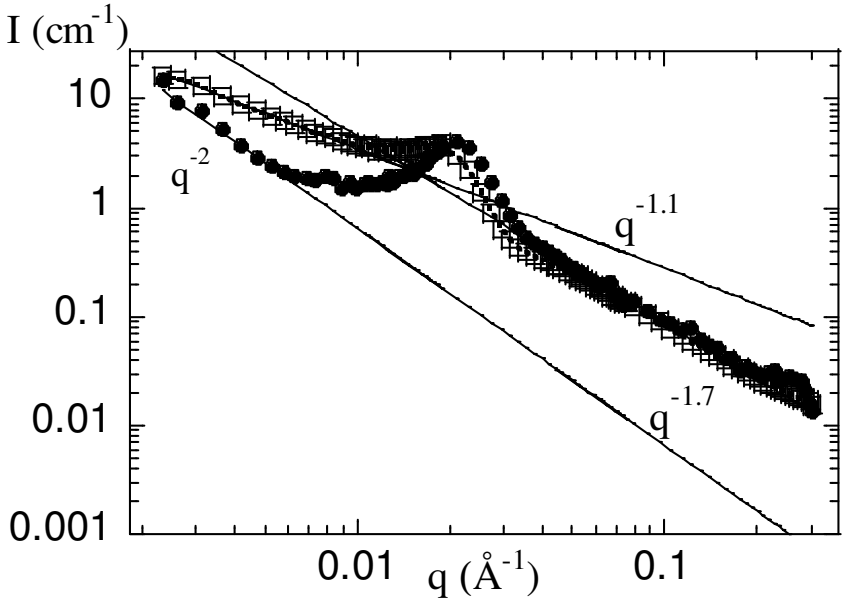

Figure 8 (Puech et al)

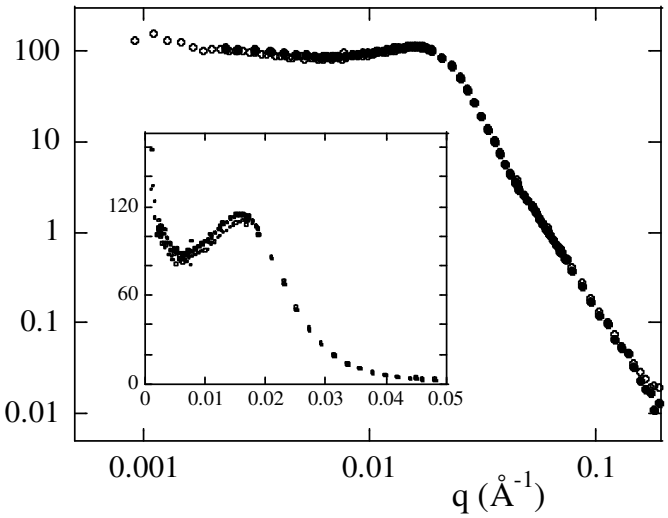

Figure 9 (Puech et al)